Environmental Science & Technology

Article

Cite This: Environ. Sci. Technol. 2018, 52, 5378−5385

pubs.acs.org/est

Activation of Periodate by Freezing for the Degradation of Aqueous Organic Pollutants

Yejin Choi,[†] Ho-Il Yoon,[‡] Changha Lee,[§] L'ubica Vetráková,[∥] Dominik Heger,[∥] Kitae Kim,[*,‡,⊥] and Jungwon Kim[*,†]

[†]Department of Environmental Sciences and Biotechnology, Hallym University, Chuncheon, Gangwon-do 24252, Republic of Korea

[‡]Korea Polar Research Institute (KOPRI), Incheon 21990, Republic of Korea

[§]School of Urban and Environmental Engineering, Ulsan National Institute of Science and Technology (UNIST), Ulsan 44919, Republic of Korea

[∥]Department of Chemistry and Research Centre for Toxic Compounds in the Environment (RECETOX), Faculty of Science, Masaryk University, Kamenice 5, 625 00 Brno, Czech Republic

[⊥]Department of Polar Sciences, University of Science and Technology (UST), Incheon 21990, Republic of Korea

Supporting Information

ABSTRACT: A new strategy (i.e., freezing) for the activation of IO_4^- for the degradation of aqueous organic pollutants was developed and investigated. Although the degradation of furfuryl alcohol (FFA) by IO_4^- was negligible in water at 25 °C, it proceeded rapidly during freezing at −20 °C. The rapid degradation of FFA during freezing should be ascribed to the freeze concentration effect that provides a favorable site (i.e., liquid brine) for the proton-coupled degradation process by concentrating IO_4^-, FFA, and protons. The maximum absorption wavelength of cresol red (CR) was changed from 434 nm (monoprotonated CR) to 518 nm (diprotonated CR) after freezing, which confirms that the pH of the aqueous IO_4^- solution decreases by freezing. The degradation experiments with varying experimental parameters demonstrate that the degradation rate increases with increasing IO_4^- concentration and decreasing pH and freezing temperature. The application of the IO_4^-/freezing system is not restricted to FFA. The degradation of four other organic pollutants (i.e., tryptophan, phenol, 4-chlorophenol, and bisphenol A) by IO_4^-, which was negligible in water, proceeded during freezing. In addition, freezing significantly enhanced the IO_4^--mediated degradation of cimetidine. The outdoor experiments performed on a cold winter night show that the IO_4^-/freezing system for water treatment can be operated without external electrical energy.

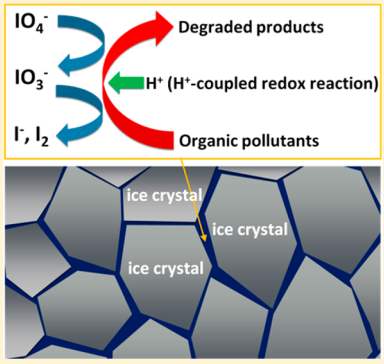

INTRODUCTION

Inorganic periodate (IO_4^-) has been used for the oxidation of various organic compounds, such as polysaccharides, alginates, amino compounds, and phenolic compounds.[1−5] However, the application of IO_4^- as a chemical oxidant for water treatment is limited because the IO_4^--mediated oxidation process is usually very slow. To enhance the oxidation ability of IO_4^-, a variety of techniques for IO_4^- activation have been employed including a UV/IO_4^- system,[6,7] an ultrasound/IO_4^- system,[8] a bimetallic nanoparticle/IO_4^- system,[9] and a KOH/IO_4^- system.[10] Short wavelength UV ($\lambda \leq 266$ nm) or ultrasound irradiation of IO_4^- generates powerful oxidants such as iodyl ($IO_3^{\bullet}$) and hydroxyl ($^{\bullet}OH$) radicals (reactions 1 and 2). The presence of bimetallic nanoparticles (Fe^0/Ni or Fe^0/Cu) converts IO_4^- to $IO_3^{\bullet}$ directly or indirectly through the formation of $H^{\bullet}$ (reactions 3−5). The reaction between IO_4^- and OH^- produces reactive oxygen species (ROS) such as the superoxide radical ($O_2^{\bullet-}$) and singlet oxygen ($^1O_2$) (reactions 6 and 7).

$$IO_4^- + \text{UV light (or ultrasound)} \rightarrow IO_3^{\bullet} + O^{\bullet-} \quad (1)$$

$$O^{\bullet-} + H^+ \rightarrow {}^{\bullet}OH \quad (2)$$

$$2IO_4^- + \text{bimetallic nanoparticle} + 4H^+ \rightarrow 2IO_3^{\bullet} + \text{bimetallic nanoparticle}^{2+} + 2H_2O \quad (3)$$

$$\text{bimetallic nanoparticle} + 2H^+ \rightarrow \text{bimetallic nanoparticle}^{2+} + 2H^{\bullet} \quad (4)$$

$$IO_4^- + H^{\bullet} \rightarrow IO_3^{\bullet} + OH^- \quad (5)$$

$$3IO_4^- + 2OH^- \rightarrow 3IO_3^- + 2O_2^{\bullet-} + H_2O \quad (6)$$

$$2O_2^{\bullet-} + 2H_2O \rightarrow {}^1O_2 + H_2O_2 + 2OH^- \quad (7)$$

The activation of IO_4^- generates powerful oxidants such as $IO_3^{\bullet}$, $^{\bullet}OH$, $O_2^{\bullet-}$, and $^1O_2$, which facilitates the application of IO_4^- for

Received: January 16, 2018
Revised: April 11, 2018
Accepted: April 12, 2018
Published: April 12, 2018

DOI: 10.1021/acs.est.8b00281
Environ. Sci. Technol. 2018, 52, 5378−5385

water treatment by increasing the degradation rate of aquatic pollutants.

Chemical reactions at temperatures below the freezing point are usually slower than those at temperatures above the freezing point. Therefore, food and unstable chemicals are put in a freezer for long-term storage. However, specific chemical reactions are significantly accelerated during the freezing process due to the existence of thin liquid layer among the solid ice crystals (i.e., ice−ice interface) and on the solid ice crystals (i.e., ice−air interface) at temperatures between the freezing and eutectic points.[11−14] Various terminologies such as liquid brine, ice grain boundary, micropocket have been used to denote this confined liquid layer at temperatures below the freezing point. Solutes and dissolved gases in aqueous solution are expelled from the growing ice crystals and concentrated in the shrinking liquid brine during freezing.[15−17] In addition, protons and hydroxides are accumulated in the liquid brine under acidic and basic conditions, respectively.[18] Therefore, an acidic solution becomes more acidic and a basic solution becomes more basic by freezing. The concentration of solutes, dissolved gases, and protons/hydroxides in the liquid brine during freezing is referred as the "freeze concentration effect".

This freeze concentration effect during freezing can enhance the chemical reactions in the cold space by increasing the concentrations of reactants and constituting a favorable condition for chemical reactions (i.e., oxygen-rich condition and/or extremely acidic/basic condition). In addition, the reductive/oxidative conversions of pollutants (i.e., chemical reactions between the pollutants or between the pollutants and natural matters) can be accelerated in the cryosphere (e.g., permafrost, polar regions, high-latitudes, and midlatitudes during the winter season). The oxidation rate of nitrite (NO_2^-) to nitrate (NO_3^-) in the presence of oxygen increased by approximately 10^5 times upon freezing.[19,20] The redox conversions between chromate (Cr^{6+}) and hydrogen peroxide (H_2O_2)[21]/arsenite (As^{3+})[22]/phenolic pollutants[23]/NO_2^-[24] were significantly enhanced during freezing. The reduction of bromate (BrO_3^-) by humic substances, which was negligible in water, was clearly observed when the solution was frozen.[25] The *N*-nitrosation reaction of dimethylamine with NO_2^- was significantly accelerated by freezing.[26] Recently, the freezing process was applied to water treatment, in which the NO_2^--mediated oxidation of sulfamethoxazole was significantly accelerated by freezing.[27]

Although various methods for the activation of IO_4^- have been developed and applied to the degradation of aquatic pollutants,[6−10] the freezing process has not been tried to activate IO_4^-. The term "activation of IO_4^-" usually refers to "the conversion of IO_4^- to oxidizing species such as $IO_3^\bullet$ and reactive oxygen species". However, in a broad sense, the term "activation of IO_4^-" in this study has been used to refer to "providing a reaction medium in which IO_4^- itself favorably acts as an oxidizing species". Herein, we report a new strategy for the activation of IO_4^- and its application for water treatment, that is, the degradation of aqueous organic pollutants in the presence of IO_4^- by freezing. The degradation of organic pollutants with the simultaneous conversion of IO_4^- during freezing at −20 °C was investigated and compared with that in water at 25 °C. The freezing-induced degradation of organic pollutants in the presence of IO_4^- was measured as a function of various experimental parameters, such as IO_4^- concentration, pH, and freezing temperature. The degradation kinetics of various organic pollutants, such as furfuryl alcohol, cimetidine, tryptophan, phenol, 4-chlorophenol, and bisphenol A, in the IO_4^-/freezing system was compared. Outdoor experiments were performed to verify the practical viability of the IO_4^-/freezing system for water treatment (i.e., the energy-free IO_4^-/freezing system in cold regions). Furthermore, the degradation mechanism of organic pollutants by IO_4^- during freezing is discussed.

■ EXPERIMENTAL SECTION

Chemicals. All chemicals were used as received without further purification. They include potassium periodate (KIO_4, Sigma-Aldrich, ≥ 99.8%), potassium iodate (KIO_3, Sigma-Aldrich, ≥ 99.5%), potassium iodide (KI, Junsei, ≥ 99.5%), furfuryl alcohol (FFA, $C_5H_6O_2$, Aldrich, ≥ 98.0%), tryptophan ($C_{11}H_{12}N_2O_2$, Sigma-Aldrich, ≥ 98.0%), cimetidine ($C_{10}H_{16}N_6S$, Sigma, 100%), phenol (C_6H_5OH, Sigma-Aldrich, ≥ 99.0%), 4-chlorophenol (ClC_6H_4OH, Aldrich, ≥ 99.0%), bisphenol A ($C_{15}H_{16}O_2$, Aldrich, ≥ 99.0%), and cresol red (CR, $C_{21}H_{18}O_5S$, Sigma-Aldrich, ≥ 95.0%). All solutions were prepared with ultrapure deionized water (resistivity = 18.3 MΩ·cm) that was prepared using a Human-Power I+ water purification system (Human Corporation).

Experimental Procedure. Aliquots of IO_4^- (usually 1 mM, 10 mL) and an organic pollutant (usually FFA, 200 μM, 10 mL) stock solution were added to 80 mL of water in a beaker to yield the desired initial concentration (usually [IO_4^-] = 100 μM and [organic pollutant] = 20 μM). The pH of the solution (100 mL) was adjusted using a $HClO_4$ or NaOH solution to the desired value (usually pH 3.0). The solution was unbuffered. Ten mL of this solution was put in a polypropylene conical tube (volume = 15 mL, Nest Biotechnology). The conical tube containing the aqueous solution of IO_4^- and organic pollutant was placed in a stainless steel tube rack in a cryogenic ethanol bath, which was precooled to the desired temperature (usually −20 °C), to freeze the aqueous solution. The moment that the conical tube containing the aqueous solution was put into the cryogenic ethanol bath was defined as "reaction time zero (t = 0)". After reaction in the cryogenic ethanol bath, the conical tube containing the frozen solution was put into a water bath at 35 °C to thaw the frozen solution. The melted solution was immediately analyzed. The experiments in an ethanol bath preset at 25 °C were also performed as the control experiments. Multiple (two or more) experiments were performed for a given condition to confirm data reproducibility.

Outdoor experiments were performed on a vacant lot beside the Natural Science Building in Hallym University (Chuncheon city, Republic of Korea) (37° 89′ N, 127° 47′ E) at night on December 12, 2017. The wind blew lightly. The temperatures during the outdoor experiments were in the range of −15 ∼ −16 °C. Ten mL of aqueous solution containing IO_4^- and FFA ([IO_4^-] = 100 μM, [FFA] = 20 μM, and pH 3.0) was put in a 100 mL beaker. The beaker was set down on the outside ground.

Chemical Analyses. The concentrations of organic pollutants, such as FFA, cimetidine, tryptophan, phenol, 4-chlorophenol, and bisphenol A, were measured using high-performance liquid chromatography (HPLC, Agilent 1120) equipped with a UV−visible detector and a Zorbax 300SB C-18 column (4.6 mm × 150 mm). The eluent consisted of a binary mixture of 0.1% phosphoric acid solution and acetonitrile, and its flow rate was 1.0 mL/min. The volume ratios (0.1% phosphoric acid solution:acetonitrile) of the eluents and the detection wavelengths were as follows: 85:15 and 218 nm for FFA, 95:5 and 218 nm for cimetidine, 90:10 and 220 nm for tryptophan, 70:30 and 270 nm for phenol, 80:20 and 228 nm for 4-

DOI: 10.1021/acs.est.8b00281
Environ. Sci. Technol. 2018, 52, 5378−5385

chlorophenol, and 70:30 and 229 nm for bisphenol A, respectively. The concentration of total organic carbon (TOC) was measured using a TOC analyzer (Shimadzu TOC-L_{CPH}) equipped with a nondispersive infrared sensor as a CO_2 detector.

The quantitative analyses of IO_3^- and I^- were performed using an ion chromatograph (IC, Dionex ICS-1100) equipped with a Dionex IonPac AS-14 column (4 mm × 250 mm) and a conductivity detector. A binary mixture of 3.5 mM sodium carbonate and 1 mM sodium bicarbonate was used as the eluent at a flow rate of 1.0 mL/min. The concentration of I_2 was determined by measuring the absorbance at 460 nm (ε = 746 M^{-1} cm^{-1} at 460 nm)[28] using a UV−visible spectrophotometer (Shimadzu UV-2600). Because the absorbance at 353 nm, which is ascribed to the generation of I_3^- (ε = 26 400 M^{-1} cm^{-1} at 353 nm and ε = 975 M^{-1} cm^{-1} at 460 nm),[28] was negligible (less than 0.0015 (= 0.06 μM), see Figure S1 in the Supporting Information, SI), only I_2 is responsible for the absorbance at 460 nm.

pH Estimation of the Frozen Solution. The pH of the frozen solution was estimated by measuring the UV−visible absorption spectra of cresol red (CR) as an in situ pH probe after freezing, but without thawing (i.e., in the liquid brine).[29,30] 3 mL of an aqueous solution containing IO_4^- (100 μM) and CR (20 μM) in a cylindrical quartz tube (4 mL) was frozen at −20 °C in a cryogenic ethanol bath and its UV−visible absorption spectrum was immediately recorded using a UV−visible spectrophotometer equipped with a diffuse reflectance accessory (Agilent Cary 5000) after taking the cylindrical quartz tube out from the cryogenic ethanol bath. Nitrogen gas was continuously introduced into the sample compartment to prevent moisture condensation on the cylindrical quartz tube. Pure ice prepared in identical manner was used as a reference.

CR exists in three different forms depending on the pH and exhibits different maximum absorption wavelengths (λ_{max} = 518 nm for diprotonated CR, λ_{max} = 434 nm for monoprotonated CR, and λ_{max} = 573 nm for deprotonated CR).[31] However, the three different CR forms cannot coexist in the equilibrium state because there is a great gap between first and second acid dissociation constants (pK_a) of CR (pK_{a1} = 1.10 and pK_{a2} = 8.15).[32,33] Only diprotonated CR and monoprotonated CR or monoprotonated CR and deprotonated CR can coexist. Therefore, the relative concentrations of the two different CR forms (i.e., [monoprotonated CR]/[diprotonated CR] or [deprotonated CR]/[monoprotonated CR]) can be obtained by fitting the data in the UV−visible absorption spectra of CR to eq 8.[29,30] The non-negative least-squares minimization was performed using Matlab. The pH of frozen solution was calculated according to eq 9 using the relative concentrations of the two different CR forms obtained from eq 8 and the pK_a value.

$$\sum_{\lambda=400\text{nm}}^{650\text{nm}} (A\cdot a + B\cdot b - X)^2 = \text{minimum value} \tag{8}$$

where X stands for the absorbance of frozen solution, A and B stand for the absorbances of pure diprotonated CR and monoprotonated CR (or the absorbances of pure monoprotonated CR and deprotonated CR), respectively, and a and b (non-negative parameters) are the relative concentrations of diprotonated CR and monoprotonated CR (or the relative concentrations of monoprotonated CR and deprotonated CR), respectively.

$$\text{pH} = pK_{a1} + \log\frac{[\text{monoprotonated CR}]}{[\text{diprotonated CR}]} \left(\text{or } pK_{a2} + \log\frac{[\text{deprotonated CR}]}{[\text{monoprotonated CR}]}\right) \tag{9}$$

RESULTS AND DISCUSSION

Degradation of Furfuryl Alcohol (FFA) by IO_4^- during Freezing. The degradation of FFA as a model organic pollutant in the presence of IO_4^- during freezing at −20 °C was investigated (Figure 1a). The degradation of FFA by IO_4^-

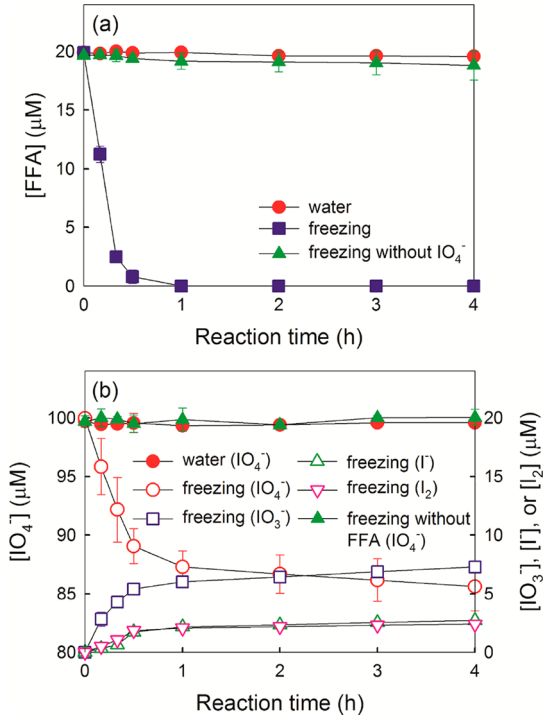

Figure 1. (a) Degradation of FFA in the presence of IO_4^- and (b) the concurrent production of IO_3^-, I^-, and I_2 in water and during freezing. Experimental conditions were as follows: [IO_4^-] = 100 μM, [FFA] = 20 μM, pH 3.0, water temperature = 25 °C, and freezing temperature = −20 °C.

proceeded rapidly during freezing. The degradation of FFA was initiated after 6 min (i.e., when the aqueous solution was almost solidified) (see SI Figures S2 and S3). After 6 min of induction period, the concentration of FFA gradually decreased with the reaction time, and FFA was completely degraded after 1 h of reaction. The mineralization (i.e., the TOC removal) efficiency was 13.5 (±1.2)% after 4 h of reaction. However, FFA was not degraded by IO_4^- in water at 25 °C. In addition, the degradation of FFA during freezing was negligible in the absence of IO_4^-. The results of the control experiments without either freezing or IO_4^- indicate that both freezing and IO_4^- are required for the degradation of FFA.

The degradation of FFA by IO_4^- during freezing was accompanied by the reduction of IO_4^- by FFA. The generation of IO_3^-, I^-, and I_2 was observed in both the presence of IO_4^- and FFA during freezing (Figure 1b). The total iodine mass balance was satisfactory throughout the freezing reaction (i.e., reduced [IO_4^-] = generated [IO_3^-] + generated [I^-] + 2 × generated [I_2]) (see SI Figure S4). This result implies that the missing

DOI: 10.1021/acs.est.8b00281
Environ. Sci. Technol. 2018, 52, 5378−5385

iodine species are negligible. In accordance with the results of control experiments for FFA degradation, IO_4^- was not reduced in the absence of either FFA or freezing (Figure 1b).

Activation Mechanism of IO_4^- by Freezing. IO_4^- exists in various forms, such as H_5IO_6, $H_4IO_6^-$, $H_3IO_6^{2-}$, $H_2IO_6^{3-}$, IO_4^-, and $H_2I_2O_{10}^{4-}$, in water and their molar fraction depends on the pH and the concentration of IO_4^- (see SI eqs S1−S5).[34] The speciation of IO_4^- can be changed during freezing because the concentration of IO_4^- increases and the pH decreases (at acidic conditions) by a freeze concentration effect that accumulates IO_4^- and protons in the liquid brine. It was previously estimated that the solute concentration increases by 10^3−10^6 times[15] and the pH decreases (at acidic conditions) by 2−4 during freezing.[18] Due to the increase in IO_4^- concentration and decrease in pH by freezing, the main iodine^{VII} species in water and during freezing can be different. To estimate the main iodine^{VII} species in water and during freezing, the pH-dependent speciation of IO_4^- was calculated at $[IO_4^-]$ = 100 μM, 100 mM, and 100 M using the MINEQL+ chemical equilibrium modeling system (SI Figure S5). Only IO_4^- is dominant in water under experimental conditions identical to those of Figure 1 (i.e., at pH 3.0 and $[IO_4^-]$ = 100 μM) (see the results at pH 3.0 in SI Figure S5a). However, both IO_4^- and H_5IO_6 are expected as a main species during freezing assuming that IO_4^- and protons are concentrated in the liquid brine by 10^3−10^6 and 10^2−10^4 times, respectively (see the results in the pH range of 0−1 in SI Figures S5b and c).

Although IO_4^- and H_5IO_6 have a fairly high oxidation power (standard reduction potentials (E^0) of IO_4^- and H_5IO_6 = 1.623 and 1.601 V_{NHE}, respectively),[35] protons are essentially required in the degradation process, as shown in reactions 10 and 11. The negligible degradation of FFA by IO_4^- in water at pH 3.0 (Figure 1a) implies that 1 mM of protons is not sufficient to drive the degradation of FFA. However, protons are concentrated in the liquid brine by exclusion from ice crystals during freezing, which makes the liquid brine a favorable site for the proton-coupled degradation process (reactions 10 and 11). That is, the degradation of FFA by IO_4^- during freezing is most likely due to the pH decrease by the freeze concentration effect. The generation of IO_3^- as a product of IO_4^- reduction indirectly supports this scenario (see Figure 1b and reactions 10 and 11). Not only IO_3^- but also I^- and I_2 were generated during the freezing-induced degradation of FFA in the presence of IO_4^- (Figure 1b). This result indicates that IO_3^- (E^0 = 1.085 or 1.195 V_{NHE})[35] generated from IO_4^- reduction is also involved in the degradation of FFA during freezing (reactions 12 and 13). When IO_3^- was used instead of IO_4^-, the degradation of FFA was also observed during freezing (see SI Figure S6).

$$IO_4^- + 2H^+ + 2e^- \rightarrow IO_3^- + H_2O,\ E^0 = 1.623V_{NHE} \quad (10)$$

$$H_5IO_6 + H^+ + 2e^- \rightarrow IO_3^- + 3H_2O,\ E^0 = 1.601V_{NHE} \quad (11)$$

$$IO_3^- + 6H^+ + 6e^- \rightarrow I^- + 3H_2O,\ E^0 = 1.085V_{NHE} \quad (12)$$

$$IO_3^- + 6H^+ + 5e^- \rightarrow 0.5I_2 + 3H_2O,\ E^0 = 1.195V_{NHE} \quad (13)$$

However, the degradation of FFA by I_2 as well as by I^- was negligible both in water and during freezing (SI Figure S7), which indicates that I^- and I_2 generated from IO_3^- reduction had little involvement in the degradation of FFA. The one-electron reduction of IO_4^- generates $IO_3^\bullet$, which is a highly reactive oxidant ($IO_4^- + 2H^+ + e^- \rightarrow IO_3^\bullet + H_2O$).[9,36] If the one-electron transfer from FFA to IO_4^- during freezing is kinetically favored, FFA can be degraded not only through the electron transfer mechanism (reactions 10−13) but also through radical mechanism. However, the $IO_3^\bullet$-mediated degradation of FFA is only conjecture at this point.

To investigate whether the pH of the aqueous IO_4^- solution really decreases and how much (if any) does the pH decrease by freezing, the UV−visible absorption spectra of cresol red (CR) as an in situ pH probe were measured before and after freezing the aqueous IO_4^- solution containing CR. The maximum absorption wavelength (λ_{max}) of CR varies according to the pH-dependent type of CR (λ_{max} = 518 nm for diprotonated CR, λ_{max} = 434 nm for monoprotonated CR, and λ_{max} = 573 nm for deprotonated CR).[31] The maximum absorbance of CR in aqueous IO_4^- solution at pH 3.0 was observed at 434 nm (SI Figure S8) because only monoprotonated CR, which exhibits λ_{max} at 434 nm, exists at pH 3.0 (see SI Figure S9). The λ_{max} of CR was shifted from 434 to 518 nm (i.e., most monoprotonated CR was changed to diprotonated CR) after freezing (SI Figure S8), which indicates that the pH of aqueous IO_4^- solution decreased by freezing. The ratio of [monoprotonated CR] to [diprotonated CR] after freezing was obtained from SI Figure S8 and eq 8 and estimated to be approximately 1 to 7.1 (i.e., [monoprotonated CR]/[diprotonated CR] = 0.14). Based on eq 9, the pH of the frozen IO_4^- solution was estimated to be approximately 0.2. The pH decrease from 3.0 to 0.2 by freezing is consistent with the previous result that the pH decreases by 2−4 by freezing.[18]

To provide convincing evidence that supports the activation of IO_4^- by the freezing-induced pH decrease, the degradation of FFA in water was investigated at high concentration of IO_4^- and/or low pH (Figure 2). The degradation of FFA in water was negligible at $[IO_4^-]$ = 100 μM and pH 3.0. An increase in the IO_4^- concentration by 100 times (100 μM → 10 mM) at pH 3.0 also did not induce the degradation of FFA. However, the degradation of FFA in water proceeded when the pH decreased by 2 (3.0 → 1.0) at $[IO_4^-]$ = 100 μM. This result clearly indicates that the pH decrease by freezing is primarily responsible for the degradation of FFA by IO_4^-. The degradation of FFA at pH 1.0 was accelerated when the concentration of IO_4^- increased by 100 times (100 μM → 10 mM). Overall, the decrease in pH and the increase in the IO_4^- concentration in liquid brine by freezing facilitates the proton-coupled degradation processes (reactions

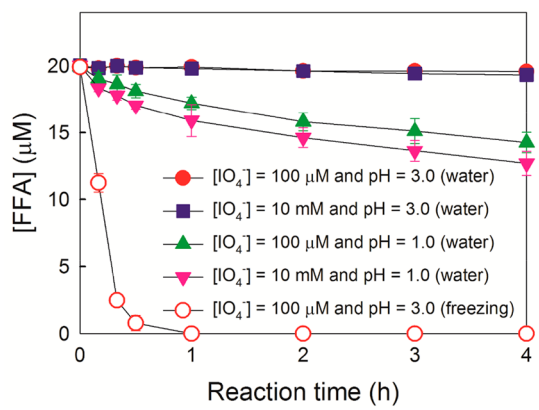

Figure 2. Effect of IO_4^- concentration increase and/or pH decrease on the degradation of FFA by IO_4^- in water. Experimental conditions were as follows: $[IO_4^-]$ = 100 μM or 10 mM, [FFA] = 20 μM, pH 3.0 or 1.0, water temperature = 25 °C, and freezing temperature = −20 °C.

DOI: 10.1021/acs.est.8b00281
Environ. Sci. Technol. 2018, 52, 5378−5385

10−13) and enhances the degradation kinetics, respectively. It should be noted that the degradation of FFA during freezing at $[IO_4^-]$ = 100 μM and pH 3.0 was much faster than that in water at $[IO_4^-]$ = 10 mM and pH 1.0 (practically possible limit). This should be because freezing increases the concentrations of IO_4^- and protons in the liquid brine much greater than 100 times. In addition, the concentration of FFA in liquid brine should also increase during freezing, which increases the degradation rate of FFA by increasing the chance of contact between IO_4^- and FFA.

Freezing-Induced Degradation of FFA in the Presence of IO_4^- under Various Conditions. The effect of IO_4^- concentration, pH, and freezing temperature on the IO_4^--mediated degradation of FFA during freezing was investigated (Figure 3). The degradation of FFA by IO_4^- in water was negligible under experimental conditions identical to those of Figure 3 except for the reaction temperature. The degradation rate of FFA during freezing increased with increasing IO_4^- concentration (Figure 3a). Even 12.5 μM of IO_4^- completely degraded 20 μM of FFA, which should be ascribed to the fact that IO_3^- generated from IO_4^- reduction is also involved in the degradation of FFA. All previous methods for the activation of IO_4^- (i.e., a UV/IO_4^- system, an ultrasound/IO_4^- system, a bimetallic nanoparticle/IO_4^- system, and a KOH/IO_4^- system) require high concentrations of IO_4^- because they cannot further activate IO_3^- that is generated from IO_4^- conversion (the concentration of the degraded pollutant is less than the concentration of added IO_4^-).[6−10] On the other hand, the freezing method can activate not only IO_4^- but also IO_3^-, which reduces the dose of IO_4^- for water treatment (the concentration of the degraded pollutant is higher than the concentration of added IO_4^-).

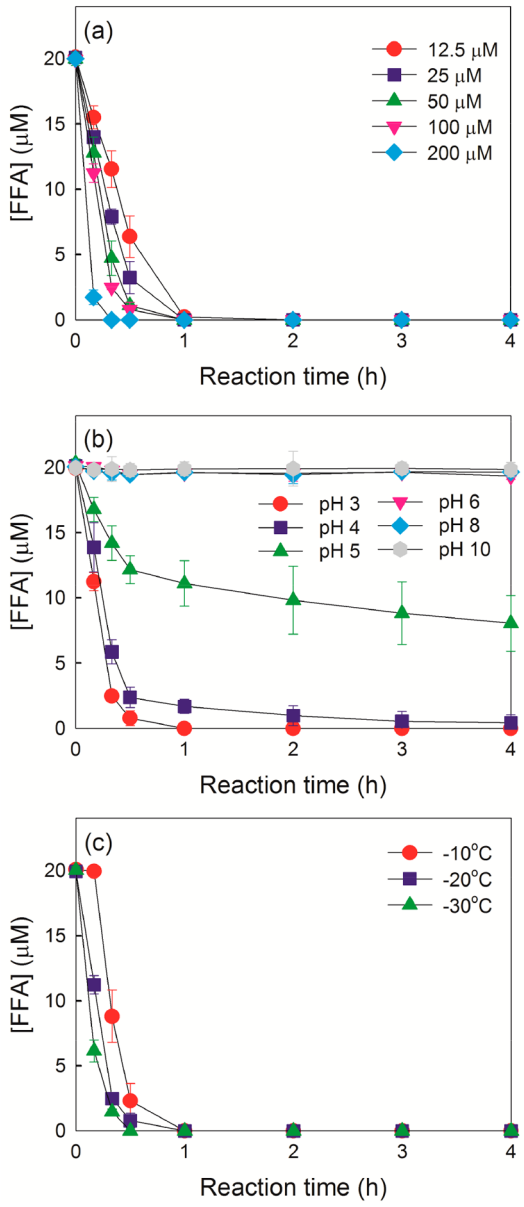

Figure 3. Effect of (a) IO_4^- concentration, (b) pH, and (c) freezing temperature on the IO_4^--mediated degradation of FFA during freezing. Experimental conditions were as follows: $[IO_4^-]$ = 100 μM for parts b and c, [FFA] = 20 μM, pH 3.0 for parts a and c, and freezing temperature = −20 °C for parts a and b.

Figure 3b shows the pH-dependent degradation kinetics of FFA in the presence of IO_4^- during freezing. The degradation of FFA was observed below pH 5.0 but was negligible above pH 6.0. The pH of the aqueous IO_4^- solution at $[IO_4^-]$ = 100 μM and under acidic conditions decreases by 2.8 after freezing (see SI Figure S8 and accompanying discussion). Freezing can reduce the pH from 6.0 to 3.2, which is still an unfavorable condition for the activation of IO_4^- (see Figure 2). Therefore, FFA was not degraded during freezing at the acidic pH 6.0. Under basic conditions, hydroxides are accumulated, and the pH increases in the liquid brine by freezing, which constitutes a more unfavorable condition for the proton-coupled degradation process. In the pH range of 3−5, the degradation of FFA by IO_4^- during freezing was accelerated as the pH decreased. This behavior is because the lower pH provides a better condition for the proton-coupled degradation process.

We also investigated the effect of freezing temperature on the degradation of FFA by IO_4^- (Figure 3c). The degradation rate of FFA increased with decreasing freezing temperature. The generation of IO_3^-, I^-, and I_2 as products of IO_4^- and IO_3^- reduction was also accelerated with decreasing freezing temperature (SI Figure S10). The concentrations of IO_4^-, FFA, and protons in the liquid brine gradually increase with an increase in the size of ice crystals (i.e., with decreasing volume of liquid brine) during freezing. The larger size of ice crystals (i.e., the smaller volume of liquid brine) at lower freezing temperatures produces higher concentrations of IO_4^-, FFA, and protons in the liquid brine at any reaction time. Overall, a lower freezing temperature increases the degradation rate of FFA by more rapidly concentrating IO_4^-, FFA, and protons in liquid brine.

Applicability of the IO_4^-/Freezing System for Water Treatment. To verify the applicability of the IO_4^-/freezing system for water treatment, the freezing-induced degradation of FFA in the presence of IO_4^- was repeated up to 20 cycles in the same batch by thawing the frozen sample and injecting FFA every 30 min (Figure 4). When IO_4^- (100 μM) was added only at the beginning of first cycle, the nearly complete degradation of FFA (20 μM) was achieved up to 10 cycles but was reduced from 11th cycle (Figure 4a). Because 10 μM of IO_4^- is consumed for the degradation of 20 μM of FFA (see Figure 1), 100 μM of IO_4^- should be completely consumed after 10 cycles. Therefore, the reduced degradation efficiency of FFA from 11th cycle should be due to the complete depletion of IO_4^-. Although IO_3^-, I^-, and I_2 remain after 10 cycles, only IO_3^- can act as an oxidant (see SI Figures S6 and S7). Therefore, the degradation of FFA after 10th cycle (i.e., even in the absence of IO_4^-) should be due to the

DOI: 10.1021/acs.est.8b00281
Environ. Sci. Technol. 2018, 52, 5378−5385

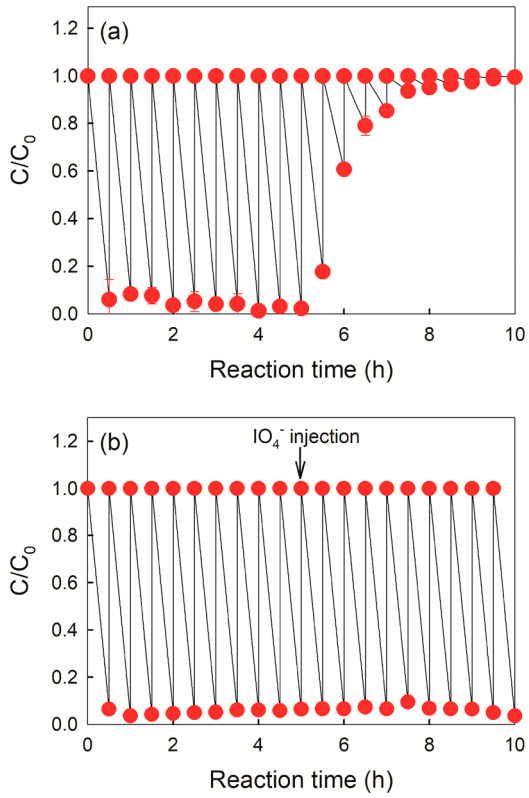

Figure 4. Repeated cycles of FFA degradation by IO_4^- during freezing. FFA was injected at the beginning of each cycle (i.e., every 30 min). For part a, IO_4^- was added only at the beginning of first cycle. For part b, IO_4^- was additionally injected at the beginning of 11th cycle. Experimental conditions were as follows: initial and injected $[IO_4^-]$ = 100 μM, initial and injected [FFA] = 20 μM, pH 3.0, and freezing temperature = −20 °C.

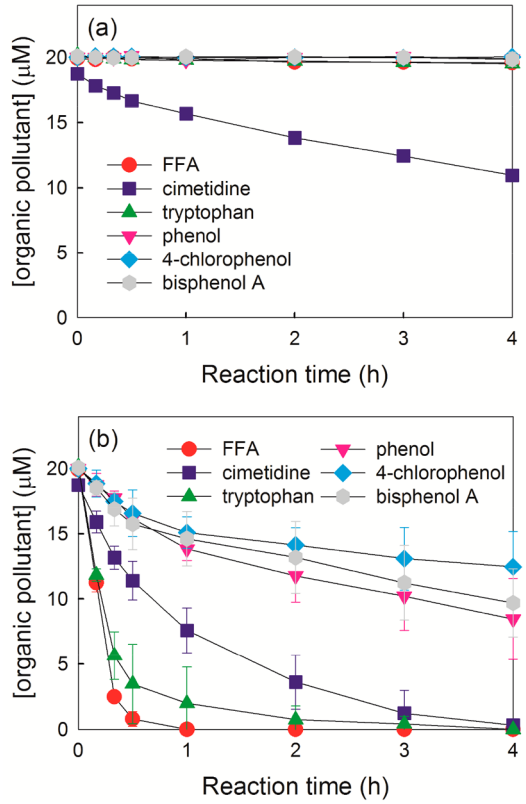

Figure 5. Time profiles of the degradation of various organic pollutants (FFA, cimetidine, tryptophan, phenol, 4-chlorophenol, and bisphenol A) by IO_4^- (a) in water and (b) during freezing. Experimental conditions were as follows: $[IO_4^-]$ = 100 μM, [organic pollutant] = 20 μM, pH 3.0, water temperature = 25 °C, and freezing temperature = −20 °C.

residual IO_3^-. However, the additional injection of IO_4^- at the beginning of 11th cycle maintained the degradation efficiency of FFA constant up to 20 cycles (Figure 4b). A stable degradation efficiency throughout the repeated cycles before the complete depletion of IO_4^- makes the IO_4^-/freezing system a practical alternative for water treatment.

We also investigated the degradation of other organic pollutants (i.e., pharmaceutical and phenolic compounds), which are frequently used to evaluate a new water treatment system,[37,38] in the IO_4^-/freezing system (Figure 5). Cimetidine and tryptophan were selected as pharmaceutical pollutants. Phenolic pollutants used in this study include phenol, 4-chlorophenol, and bisphenol A. Although the degradation rate of the other organic pollutants during freezing was lower than that of FFA, the degradation of all organic pollutants tested in this study was clearly observed during freezing. The degradation of cimetidine by IO_4^- was observed even in water because it is very weak against the electrophilic oxidation (Figure 5a).[10] However, even if that was the case, freezing significantly accelerated the degradation of cimetidine (Figure 5b). The degradation of tryptophan, phenol, 4-chlorophenol, and bisphenol A by IO_4^-, which was negligible in water (Figure 5a), continuously proceeded during freezing (Figure 5b). In contrast to the KOH/IO_4^- system that is highly pollutant-specific,[10] the IO_4^-/freezing system can be used for the degradation of various organic pollutants. This nonselective degradation ability of the IO_4^-/freezing system improves its applicability for water treatment.

To identify which organic pollutant (i.e., chemical structure) is more effectively degraded in the IO_4^-/freezing system, the degradation rate of various substituted phenols, such as phenol, 4-chlorophenol, 2-chlorophenol, 4-bromophenol, 2-nitrophenol, 4-nitrophenol, 4-methylphenol, and 2,4-dimethylphenol, was plotted against the Hammett constant (σ^+), which quantitatively represents the electronic distribution of the substituted phenols. The degradation rates of the substituted phenols decreased with increasing Hammett constant (SI Figure S11). This negative Hammett slope signifies that the degradation of more electron-rich organic pollutants proceeds more rapidly in the IO_4^-/freezing system.

The IO_4^-/freezing system for water treatment can be operated without external electrical energy in cold regions such as high-latitudes and midlatitudes during the winter season. The freezing-induced degradation of organic pollutants in the presence of IO_4^- was tested outdoors without using a cryogenic ethanol bath (external electrical energy) to confirm the energy-free IO_4^-/freezing system. The beaker containing the aqueous solution of IO_4^- and FFA was only set down on the ground on a cold winter night in the Republic of Korea (−15 ∼ −16 °C). In contrast to laboratory experiments, which were performed in a cryogenic ethanol bath, an induction period (i.e., the time required for initiation of the degradation process) was clearly observed during the outdoor experiments. This behavior should be due to the difference between cooling methods (the ethanol

DOI: 10.1021/acs.est.8b00281
Environ. Sci. Technol. 2018, 52, 5378−5385

cooling system for the laboratory experiments vs an air cooling system for the outdoor experiments, see Discussion on the effect of cooling method on the induction period in the SI for details). The degradation of FFA was started after 1 h and completed within 2 h. (Figure 6). FFA was not degraded in the absence of

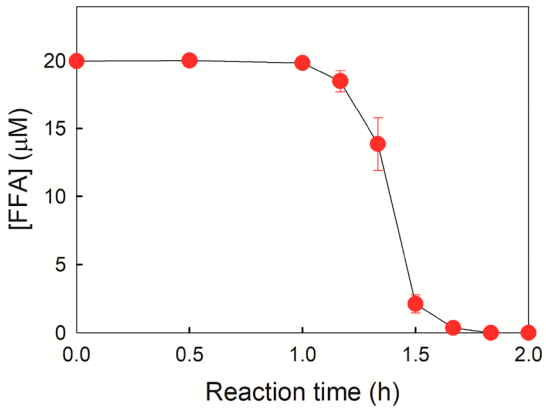

Figure 6. Degradation of FFA in the presence of IO_4^- during freezing (outdoor experiments on a cold winter night in the Republic of Korea). Experimental conditions were as follows: $[IO_4^-] = 100\ \mu M$, $[FFA] = 20\ \mu M$, pH 3.0, and temperature = −15 ∼ −16 °C.

IO_4^- under the same conditions. The outdoor experimental results propose that the IO_4^-/freezing system for water treatment is economically feasible in cold regions.

The IO_4^-/freezing system using the artificial freezing method for wastewater treatment may be impractical, because the electrical costs of freezing a large quantity of wastewater will be too high. However, the practical viability of the IO_4^-/freezing system can be established by using a natural freezing method in cold regions, because only IO_4^-, which is a cheap reagent, is required in this case. If wastewater containing IO_4^- is sprayed in the form of small drops using injection nozzles, the degradation process should be immediately initiated without an induction period due to rapid solidification. This method would make the IO_4^-/freezing system for wastewater treatment economically feasible. However, it should be noted that I^- in water treated by the IO_4^-/freezing system may contribute to the formation of toxic iodine-containing products in the chlorine (or manganese dioxide)-mediated oxidation process.[39,40] Therefore, the subsequent cost-effective methods for the removal of iodide, such as adsorption, precipitation, membrane, and ion-exchange,[41−44] should be employed in conjunction with the IO_4^-/freezing system as needed.

We investigated the degradation of aqueous organic pollutants by IO_4^- during freezing. Although the degradation of most organic pollutants was negligible in water, it proceeded rapidly during freezing. This unique behavior observed during freezing is due to a freeze concentration effect that provides a favorable site (i.e., liquid brine) for the proton-coupled degradation (i.e., the proton-coupled electron transfer) process by concentrating IO_4^-, organic pollutants, and protons in the liquid brine among the ice crystals. The electron transfer from organic pollutants to IO_4^- during freezing results in the degradation of organic pollutants accompanied by the production of IO_3^-. IO_3^- is further converted to I^- and I_2 as a result of electron transfer from organic pollutants to IO_3^-. Because freezing can activate not only IO_4^- but also IO_3^- generated from IO_4^- reduction, the freezing method can degrade more organic pollutants than other methods for IO_4^- activation at the same IO_4^- dose. The degradation efficiency of the IO_4^-/freezing system is stable throughout the repeated cycles before IO_4^- is completely depleted. The IO_4^-/freezing system can degrade a variety of organic pollutants (i.e., its application is not restricted to a specific pollutant). In particular, the IO_4^-/freezing system has the potential to be more economical in cold regions because external electrical energy for freezing is not required.

■ ASSOCIATED CONTENT

Supporting Information

The Supporting Information is available free of charge on the ACS Publications website at DOI: 10.1021/acs.est.8b00281.

Equations S1−S5, supplementary figures (S1−S11), and discussion on the effect of cooling method on the induction period (PDF)

■ AUTHOR INFORMATION

Corresponding Authors

*(K.K.) Phone: +82-32-760-5365; e-mail: ktkim@kopri.re.kr.
*(J.K.) Phone: +82-33-248-2156; e-mail: jwk@hallym.ac.kr.

ORCID

Dominik Heger: 0000-0002-6881-8699
Kitae Kim: 0000-0003-0803-3547
Jungwon Kim: 0000-0001-7804-7587

Notes

The authors declare no competing financial interest.

■ ACKNOWLEDGMENTS

Funding for this work was provided by the Korea Polar Research Institute (KOPRI) project (PE18200 and PE17560). This research was also supported by Young Research Program (NRF-2016R1A1A1A05005200), Space Core Technology Development Program (NRF-2014M1A3A3A02034875), and Basic Core Technology Development Program for the Oceans and the Polar Regions (NRF-2015M1A5A1037243) through the National Research Foundation of Korea (NRF) funded by the Ministry of Science and ICT.

■ REFERENCES

(1) Kristiansen, K. A.; Potthast, A.; Christensen, B. E. Periodate oxidation of polysaccharides for modification of chemical and physical properties. *Carbohydr. Res.* **2010**, *345*, 1264−1271.

(2) Coseri, S.; Biliuta, G.; Zemljič, L. F.; Srndovic, J. S.; Larsson, P. T.; Strnad, S.; Kreže, T.; Naderi, A.; Lindström, T. One-shot carboxylation of microcrystalline cellulose in the presence of nitroxyl radicals and sodium periodate. *RSC Adv.* **2015**, *5*, 85889−85897.

(3) Kristiansen, K. A.; Tomren, H. B.; Christensen, B. E. Periodate oxidized alginates: depolymerization kinetics. *Carbohydr. Polym.* **2011**, *86*, 1595−1601.

(4) Clamp, J. R.; Hough, L. Some observations on the periodate oxidation of amino compounds. *Biochem. J.* **1966**, *101*, 120−126.

(5) Kamimura, A.; Nokubi, T.; Nasu, K.; Takechi, Y.; Ishihara, Y.; Kato, K.; Noguchi, S.; Watanabe, M.; Shirai, M.; Sumimoto, M.; Uno, H. Facile synthesis of quinone dimer derivatives substituted with sulfanyl groups and their properties. *Chem. Lett.* **2012**, *41*, 950−951.

(6) Chia, L.-H.; Tang, X.; Weavers, L. K. Kinetics and mechanism of photoactivated periodate reaction with 4-chlorophenol in acidic solution. *Environ. Sci. Technol.* **2004**, *38*, 6875−6880.

(7) Lee, C.; Yoon, J. Application of photoactivated periodate to the decolorization of reactive dye: reaction parameters and mechanism. *J. Photochem. Photobiol., A* **2004**, *165*, 35−41.

DOI: 10.1021/acs.est.8b00281
Environ. Sci. Technol. 2018, 52, 5378−5385

(8) Lee, Y.-C.; Chen, M.-J.; Huang, C.-P.; Kuo, J.; Lo, S.-L. Efficient sonochemical degradation of perfluorooctanoic acid using periodate. *Ultrason. Sonochem.* **2016**, *31*, 499−505.
(9) Lee, H.; Yoo, H.-Y.; Choi, J.; Nam, I.-H.; Lee, S.; Lee, S.; Kim, J.-H.; Lee, C.; Lee, J. Oxidizing capacity of periodate activated with iron-based bimetallic nanoparticles. *Environ. Sci. Technol.* **2014**, *48*, 8086−8093.
(10) Bokare, A. D.; Choi, W. Singlet-oxygen generation in alkaline periodate solution. *Environ. Sci. Technol.* **2015**, *49*, 14392−14400.
(11) Bartels-Rausch, T.; Jacobi, H.-W.; Kahan, T. F.; Thomas, J. L.; Thomson, E. S.; Abbatt, J. P. D.; Ammann, M.; Blackford, J. R.; Bluhm, H.; Boxe, C.; Domine, F.; Frey, M. M.; Gladich, I.; Guzmán, M. I.; Heger, D.; Huthwelker, T.; Klán, P.; Kuhs, W. F.; Kuo, M. H.; Maus, S.; Moussa, S. G.; McNeill, V. F.; Newberg, J. T.; Pettersson, J. B. C.; Roeselová, M.; Sodeau, J. R. A review of air-ice chemical and physical interactions (AICI): liquids, quasi-liquids, and solids in snow. *Atmos. Chem. Phys.* **2014**, *14*, 1587−1633.
(12) O'Concubhair, R.; Sodeau, J. R. The effect of freezing on reactions with environmental impact. *Acc. Chem. Res.* **2013**, *46*, 2716−2724.
(13) Park, S.-C.; Moon, E.-S.; Kang, H. Some fundamental properties and reactions of ice surfaces at low temperatures. *Phys. Chem. Chem. Phys.* **2010**, *12*, 12000−12011.
(14) Kong, X.; Thomson, E. S.; Papagiannakopoulos, P.; Johansson, S. M.; Pettersson, J. B. C. Water accommodation on ice and organic surfaces: insights from environmental molecular beam experiments. *J. Phys. Chem. B* **2014**, *118*, 13378−13386.
(15) Heger, D.; Jirkovský, J.; Klán, P. Aggregation of methylene blue in frozen aqueous solutions studied by absorption spectroscopy. *J. Phys. Chem. A* **2005**, *109*, 6702−6709.
(16) Grannas, A. M.; Bausch, A. R.; Mahanna, K. M. Enhanced aqueous photochemical reaction rates after freezing. *J. Phys. Chem. A* **2007**, *111*, 11043−11049.
(17) Takenaka, N.; Bandow, H. Chemical kinetics of reactions in the unfrozen solution of ice. *J. Phys. Chem. A* **2007**, *111*, 8780−8786.
(18) Heger, D.; Klánová, J.; Klán, P. Enhanced protonation of cresol red in acidic aqueous solutions caused by freezing. *J. Phys. Chem. B* **2006**, *110*, 1277−1287.
(19) Takenaka, N.; Ueda, A.; Daimon, T.; Bandow, H.; Dohmaru, T.; Maeda, Y. Acceleration mechanism of chemical reaction by freezing: the reaction of nitrous acid with dissolved oxygen. *J. Phys. Chem.* **1996**, *100*, 13874−13884.
(20) Takenaka, N.; Ueda, A.; Maeda, Y. Acceleration of the rate of nitrite oxidation by freezing in aqueous solution. *Nature* **1992**, *358*, 736−738.
(21) Kim, K.; Kim, J.; Bokare, A. D.; Choi, W.; Yoon, H.-I.; Kim, J. Enhanced removal of hexavalent chromium in the presence of H_2O_2 in frozen aqueous solutions. *Environ. Sci. Technol.* **2015**, *49*, 10937−10944.
(22) Kim, K.; Choi, W. Enhanced redox conversion of chromate and arsenite in ice. *Environ. Sci. Technol.* **2011**, *45*, 2202−2208.
(23) Ju, J.; Kim, J.; Vetráková, L'.; Seo, J.; Heger, D.; Lee, C.; Yoon, H.-I.; Kim, K.; Kim, J. Accelerated redox reaction between chromate and phenolic pollutants during freezing. *J. Hazard. Mater.* **2017**, *329*, 330−338.
(24) Kim, K.; Chung, H. Y.; Ju, J.; Kim, J. Freezing-enhanced reduction of chromate by nitrite. *Sci. Total Environ.* **2017**, *590−591*, 107−113.
(25) Min, D. W.; Choi, W. Accelerated reduction of bromate in frozen solution. *Environ. Sci. Technol.* **2017**, *51*, 8368−8375.
(26) Kitada, K.; Suda, Y.; Takenaka, N. Acceleration and reaction mechanism of the *N*-nitrosation reaction of dimethylamine with nitrite in ice. *J. Phys. Chem. A* **2017**, *121*, 5383−5388.
(27) Sun, F.; Xiao, Y.; Wu, D.; Zhu, W.; Zhou, Y. Nitrite-driven abiotic transformation of sulfonamide micropollutants during freezing process. *Chem. Eng. J.* **2017**, *327*, 1128−1134.
(28) Awtrey, A. D.; Connick, R. E. The absorption spectra of I_2, I_3^-, I^-, IO_3^-, $S_4O_6^=$ and $S_2O_3^=$. heat of the reaction $I_3^- = I_2 + I^-$. *J. Am. Chem. Soc.* **1951**, *73*, 1842−1843.
(29) Vetráková, L'.; Vykoukal, V.; Heger, D. Comparing the acidities of aqueous, frozen, and freeze-dried phosphate buffers: is there a "pH memory" effect? *Int. J. Pharm.* **2017**, *530*, 316−325.
(30) Krausková, L'.; Procházková, J.; Klašková, M.; Filipová, L.; Chaloupková, R.; Malý, S.; Damborský, J.; Heger, D. Suppression of protein inactivation during freezing by minimizing pH changes using ionic cryoprotectants. *Int. J. Pharm.* **2016**, *509*, 41−49.
(31) Rottman, C.; Grader, G.; Hazan, Y. D.; Melchior, S.; Avnir, D. Surfactant-induced modification of dopants reactivity in sol-gel matrixes. *J. Am. Chem. Soc.* **1999**, *121*, 8533−8543.
(32) Perrin, D. D. Buffers of low ionic strength for spectrophotometric p*K* determinations. *Aust. J. Chem.* **1963**, *16*, 572−578.
(33) Dean, J. A. *Lange's Handbook of Chemistry*, 14th, ed.; McGraw-Hill: New York, 1992.
(34) Weavers, L. K.; Hua, I.; Hoffmann, M. R. Degradation of triethanolamine and chemical oxygen demand reduction in wastewater by photoactivated periodate. *Water Environ. Res.* **1997**, *69*, 1112−1119.
(35) Lide, D. R. *CRC Handbook of Chemistry and Physics*, 77th, ed.; CRC Press: Boca Raton, FL, 1996.
(36) Yun, E.-T.; Yoo, H.-Y.; Kim, W.; Kim, H.-E.; Kang, G.; Lee, H.; Lee, S.; Park, T.; Lee, C.; Kim, J.-H.; Lee, J. Visible-light-induced activation of periodate that mimics dye-sensitization of TiO_2: simultaneous decolorization of dyes and production of oxidizing radicals. *Appl. Catal., B* **2017**, *203*, 475−484.
(37) Maeng, S. K.; Cho, K.; Jeong, B.; Lee, J.; Lee, Y.; Lee, C.; Choi, K. J.; Hong, S. W. Substrate-immobilized electrospun TiO_2 nanofibers for photocatalytic degradation of pharmaceuticals: the effects of pH and dissolved organic matter characteristics. *Water Res.* **2015**, *86*, 25−34.
(38) Ramasundaram, S.; Seid, M. G.; Lee, W.; Kim, C. U.; Kim, E.-J.; Hong, S. W.; Choi, K. J. Preparation, characterization, and application of TiO_2-patterned polyimide film as a photocatalyst for oxidation of organic contaminants. *J. Hazard. Mater.* **2017**, *340*, 300−308.
(39) Hua, G.; Reckhow, D. A.; Kim, J. Effect of bromide and iodide ions on the formation and speciation of disinfection byproducts during chlorination. *Environ. Sci. Technol.* **2006**, *40*, 3050−3056.
(40) Gallard, H.; Allard, S.; Nicolau, R.; von Gunten, U.; Croué, J. P. Formation of iodinated organic compounds by oxidation of iodide-containing waters with manganese dioxide. *Environ. Sci. Technol.* **2009**, *43*, 7003−7009.
(41) Zhang, X.; Gu, P.; Zhou, S.; Li, X.; Zhang, G.; Dong, L. Enhanced removal of iodide ions by nano Cu_2O/Cu modified activated carbon from simulated wastewater with improved countercurrent two-stage adsorption. *Sci. Total Environ.* **2018**, *626*, 612−620.
(42) Liu, Y.; Gu, P.; Yang, Y.; Jia, L.; Zhang, M.; Zhang, G. Removal of radioactive iodide from simulated liquid waste in an integrated precipitation reactor and membrane separator (PR-MS) system. *Sep. Purif. Technol.* **2016**, *171*, 221−228.
(43) Zhang, X.; Gu, P.; Li, X.; Zhang, G. Efficient adsorption of radioactive iodide ion from simulated wastewater by nano Cu_2O/Cu modified activated carbon. *Chem. Eng. J.* **2017**, *322*, 129−139.
(44) Hoskins, J. S.; Karanfil, T. Removal and sequestration of iodide using silver-impregnated activated carbon. *Environ. Sci. Technol.* **2002**, *36*, 784−789.

DOI: 10.1021/acs.est.8b00281
Environ. Sci. Technol. 2018, 52, 5378−5385